

## Article

# Tailoring/Tuning Properties of Polyester Urea-Urethanes through Hybridization with Titania Obtained Using the Sol–Gel Process

Dulce María González-García <sup>1</sup>, Luis María Rodríguez-Lorenzo <sup>2</sup> , Ángel Marcos-Fernández <sup>2,\*</sup> , Rodrigo Jiménez-Gallegos <sup>1</sup> , Daniela Anahí Sánchez-Téllez <sup>1</sup>  and Lucía Téllez-Jurado <sup>1,\*</sup> 

<sup>1</sup> Department of Metallurgy and Materials Engineering, ESIQIE, Instituto Politécnico Nacional, Mexico City 07738, Mexico; dgonzalezg@ipn.mx (D.M.G.-G.); rojimenezg@ipn.mx (R.J.-G.); danielatellez06@gmail.com (D.A.S.-T.)

<sup>2</sup> Institute of Polymer Science and Technology (CSIC), Juan de la Cierva, 3, 28006 Madrid, Spain; luis.rodriguez-lorenzo@ictp.csic.es

\* Correspondence: amarcos@ictp.csic.es (Á.M.-F.); ltellezj@ipn.mx (L.T.-J.)

**Abstract:** Hybrid materials have been studied because in these materials the properties of organic components, such as elasticity and biodegradability, could be combined with the properties of inorganic components, such as good biological response, thereby transforming them into a single material with improved properties. In this work, Class I hybrid materials based on polyester-urea-urethanes and titania were obtained using the modified sol–gel method. This was corroborated using the FT-IR and Raman techniques which highlighted the formation of hydrogen bonds and the presence of Ti–OH groups in the hybrid materials. In addition, the mechanical and thermal properties and degradability were measured using techniques, such as Vickers hardness, TGA, DSC, and hydrolytic degradation; these properties could be tailored according to hybridization between both organic and inorganic components. The results show that Vickers hardness increased by 20% in hybrid materials as compared to polymers; also, the surface hydrophilicity increases in the hybrid materials, improving their cell viability. Furthermore, cytotoxicity in vitro test was carried out using osteoblast cells for intended biomedical applications and they showed non-cytotoxic behavior.

**Keywords:** tailoring properties; polyester-urea-urethanes; hybrid materials; tissue engineering



**Citation:** González-García, D.M.; Rodríguez-Lorenzo, L.M.; Marcos-Fernández, Á.; Jiménez-Gallegos, R.; Sánchez-Téllez, D.A.; Téllez-Jurado, L. Tailoring/Tuning Properties of Polyester Urea-Urethanes through Hybridization with Titania Obtained Using the Sol–Gel Process. *Polymers* **2023**, *15*, 2299. <https://doi.org/10.3390/polym15102299>

Academic Editors: Antonino Morabito and Luca Valentini

Received: 15 April 2023

Revised: 9 May 2023

Accepted: 11 May 2023

Published: 13 May 2023



**Copyright:** © 2023 by the authors. Licensee MDPI, Basel, Switzerland. This article is an open access article distributed under the terms and conditions of the Creative Commons Attribution (CC BY) license (<https://creativecommons.org/licenses/by/4.0/>).

## 1. Introduction

Organic–inorganic hybrid materials may be more favorable than polymers or inorganic materials. The main advantage of organic–inorganic hybrids is that they are a single entity combining the different properties of both organic and inorganic components and as such they also present an opportunity to develop a large set of new materials with a wide spectrum of properties [1,2]. Moreover, hybridization between the organic and inorganic components offers incredible potential to create new materials with the properties needed in various advanced applications, such as tissue engineering [3].

Elastomers, such as polyurethanes (PUs), are polymer materials that exhibit good mechanical properties, tunable chemical properties, and cytocompatibility which are used in biomedical applications [4–7]. In polyester (urea-urethanes) polymers (PEUUs), the urea group shows stronger hydrogen bonds than the urethane group in polyurethanes, thus yielding better phase-separated morphology and exhibiting better mechanical properties. They are classified as a subclass of the generic polyurethane family. On the other hand, inorganic materials, i.e., ceramics and glasses, are stiff but fragile. However, ceramics, such as titania (TiO<sub>2</sub>), shows good interfacial properties with biological hosts, good corrosion resistance, lack of inflammatory response, and low cytotoxicity [8,9]. Hence, PEUUs–titania hybrids could be promising candidates in biomedical-related applications due to their great potential for tuning properties which can fit specific requirements.

The organic–inorganic hybrids based on polymers and titania have been proposed for different applications, such as PET covered with titania nanowires and nanorods for water pollutant removals with antibacterial activity [10] or self-cleaning textiles obtained using sol–gel coatings of silica and titania nanocomposites on polyester fibers with excellent behaviors [11]. Studies on TiO<sub>2</sub> and polyethylene glycol (PEG) and the influence of the PEG molecular weight on flexibility and toughness in hybrid films was studied [12]. Studies have also been carried out on transparent aromatic polyamides (aramid)-based titania hybrid films prepared using the sol–gel process with improved elastic nature and photostability of the matrix [13]. Hybrids films of polyester-based polyurethane/titania using the sol–gel method were also reported [14] which found that introducing titania into the resin increases modulus, glass transition temperature (T<sub>g</sub>), mechanical strength, abrasion resistance, hardness, and UV absorbance. Furthermore, polydimethylsiloxane (PDMS)-modified CaO–SiO<sub>2</sub>–TiO<sub>2</sub> hybrids were successfully synthesized via a sol–gel process resulting in materials that offer high ductility, low elastic modulus, and high mechanical strength [15]. Hybrids based on poly caprolactones (PCL-d)/TiO<sub>2</sub> obtained using a sol–gel process with varying proportion of the organic component have also been reported, which shows that an increase in PCL-d amounts improved cell viability [9]. Polyurethanes-TiO<sub>2</sub> (PEU-TiO<sub>2</sub>) hybrids are barely found in the literature. In previous research, we reported the preparation of (PEU-TiO<sub>2</sub>) hybrids and showed that the addition of the inorganic component into the polyurethanes matrix improves the thermal and mechanical properties and promotes the bioactivity behavior compared to the polyurethane component [16]. However, such improvements have also been obtained in poly-ester-urea-urethanes (PEUUs) using an ester-lysine as a chain extender. This type of polymer showed higher stability in PBS than polyester-urethanes PEUs, due to the prominent hydrophobicity in their surfaces [17]. To date, no studies have been reported on hybrid materials obtained with polyester-urea-urethanes (PEUU) and titania, which have potential applications in tissue engineering.

The aims of this work are to design hybrid materials based on polyester (urea-urethanes) and titania using a sol–gel process, evaluate the change in properties when this polymer is transformed into a hybrid material and analyze their potential use as biocompatible scaffolds for bone tissue regeneration.

## 2. Experimental Procedure

### 2.1. Synthesis

PEUUs/TiO<sub>2</sub> hybrid materials were prepared in two steps: (1) synthesis of polyester (urea urethanes) (PEUUs), and (2) synthesis of organic–inorganic hybrids using a modified *sol–gel* method.

The starting reagents to prepare PEUUs were as follows: (1)  $\epsilon$ -Caprolactone ( $\epsilon$ -CL, Aldrich 97%); (2) 1,6-hexamethylene diisocyanate (HMDI, Aldrich 98%); (3) L-Lysine-ethyl-ester-dihydrochloride (LYS, Aldrich 99%); (4) Triethylamine (TEA, Sigma Aldrich, St. Louis, MO, USA) and (5) N,N-Dimethylacetamide (DMac, Aldrich 99%). The starting reagents for the synthesis of hybrids were as follows: (1) Titanium (IV) butoxide (But-TiO<sub>2</sub>, Aldrich 97%); (2) hydrochloric acid (HCl, Fermont 37%); (3) isopropanol (IPA, Aldrich 99%); and (4) Tetrahydrofuran (THF, Aldrich) and deionized water. All reagents were purchased in Sigma Aldrich S.L (Madrid, Spain). The Polycaprolactone diol (PCL-d) of 1000 g/mol nominal weight was synthesized in the laboratory using the ring opening polymerization of the  $\epsilon$ -Caprolactone following the procedure described in the literature [18].

#### 2.1.1. Synthesis of the Polyester (Urea-Urethanes) (PEUUs)

The polyester (urea-urethanes) (PEUUs) were synthesized using the previously prepared PCL-d as the soft segment; three different molecular weights (530, 1000, and 2000 umas) were assayed. The hexamethylene diisocyanate (HMDI) was used as the hard segment and L-lysine-ethyl-ester-dihydrochloride (LYS) was used as the chain extender. The procedure is described in detail in a previous paper [17]. Briefly, the molar ratio of PCL-d:HMDI:LYS was adjusted to keep the weight of the hard segment at 30%. The synthe-

sis was carried out through the two-stage polymerization technique. First, the polyester (PCL-d) reaction with the 1,6-hexamethylene diisocyanate (HMDI) was carried out in a three-neck flask under an inert atmosphere at 80 °C; these conditions were maintained for three hours to obtain the prepolymer containing the isocyanate groups. Second, the polymer (PEUUs) was obtained by adding the chain extender (LYS) and the triethylamine (TEA) in correct amounts, using *N,N*-Dimethylacetamide (DMac) as solvent at 80 °C for four hours. The added volume of solvent was adequate to achieve the dissolution of polyester (urea-urethanes) (PEUUs).

### 2.1.2. Synthesis of the Hybrid Materials (THPs)

The PEUUs-based TiO<sub>2</sub> hybrids (THPs) were obtained via a modified sol–gel method using the PEUUs previously synthesized. The synthesis of the hybrid materials was carried out via in situ reaction. First, the PEUUs were dissolved using tetrahydrofuran (THF) in a three-neck flask and then the appropriate amount of titanium (IV) butoxide (But-TiO<sub>2</sub>) was added to obtain a weight ratio of 80/20 of the organic/inorganic component. After that, water, HCl, and IPA (hydrolyzer, catalyzer, and solvent, respectively) were added, and the reaction was kept under constant stirring for one hour at 80 °C. The molar ratio of H<sub>2</sub>O:HCl:IPA was 3:0.3:4.5. The final hybrid materials were slowly dried at room temperature for several days.

### 2.2. Characterization of the THPs

Structural characterization of the (THPs) was achieved using Fourier Transform Infrared Spectroscopy (FT-IR), Raman Spectroscopy, and X-Ray Diffraction (XRD). FT-IR spectra were recorded via a Bruker spectrophotometer model Tensor 21 (FT-IR, Bruker, Ettlingen, Germany), equipped with an ATR (Attenuated Total Reflectance) PIKE model MIRacle, in transmittance mode using the mid-infrared region (from 400 to 400 cm<sup>-1</sup>) and 16 scans with a resolution of 4 cm<sup>-1</sup>. Samples were analyzed in the form of dried films. Raman spectra were obtained in a Renishaw in Via Reflex equipment with a laser diode of 785 nm coupled with a microscope and a Master Renishaw CCD camera (Raman, Renishaw plc, Wotton-under-Edge, UK). XRD analysis were carried out using a D8 FOCUS diffractometer (Bruker, Billerica, MA, USA) with a graphite filter of K $\alpha$ Cu at 40 kV and 35 mA. The sweep in 2 $\theta$  was set from 5° to 60°.

The thermogravimetric analysis (TGA) was carried out in a SETARAM brand calorimeter from 25 °C to 600 °C with a heating rate of 10 °C/min. Differential Scanning Calorimetry (DSC) analysis was conducted with a Perkin Elmer equipment from –80 °C to 200 °C and a heating rate of 10 °C/min. Two heating cycles were performed and the glass transition temperature (T<sub>g</sub>) of each material was considered the second sweep.

The morphology of the THPs was characterized using a high-resolution HITACHI SU 800 microscope with a voltage of 15 kV and a working distance of 8 mm to prevent degradation of the samples due to the presence of the organic component in the hybrid.

Hydrophilicity property of the THPs was evaluated based on contact angle measurements obtained using a KSV Instruments LTD (CAM 200, KSV instrument Ltd., Helsinki, Finland) with an integrated camera CAM 200 employing the SFE CAM 2008 program. At room temperature, water was used as means of humidification.

The micro-hardness of the THPs was measured with a Leitz RZD-DO equipment (RZD-DO, Leitz, Oberkochen, Germany). The applied load was 4.809 N; the load holding time was 25 s at room temperature. The micro-hardness is reported in MPa.

### 2.3. Degradability Assay

The degradation of THPs was evaluated by immersing the samples in 20 mL of phosphate-buffered solution (PBS, pH = 7.4) at 37 ± 0.5 °C at intervals of 1, 3, 7, 14, 21, and 28 days. The pH value of PBS was registered at each test time. Additionally, the change in weight was recorded in samples dried at 37 °C at each test time. Weight loss was calculated as, %Weight loss = 100 – (W<sub>2</sub>/W<sub>1</sub>) × 100, where W<sub>2</sub> is the weight of the dried hybrid

materials after being soaked at time  $t$  and  $W_1$  is the initial weight of dried hybrids. Three replicas of samples were tested at each test time.

#### 2.4. Cytotoxicity Test

Cell viability of (THPs) was tested with osteoblast cell lines from (INNOPROT, P10979) during 24 h, using Termanox as a negative control. The MTT assay is a biochemical test used to assess the cytotoxicity of materials via qualitative measurement of cell viability and proliferation. The reagent used to produce stain is (3-[4,5-dimethyl-thiazol-2-yl]-2,5-diphenyl-tetrazolium-bromide)-sodium-succinate (MTT). The coloration changes from yellowish to blueish, suggesting reduction in the molecule by cellular mitochondrial dehydrogenase. Blue coloration is proportional to the number of living cells. Living cells can metabolize MTT, showing an indirect measure of cell viability. Three replicas of each hybrid material were tested.

#### Statistical Analysis of Cytotoxicity

The statistical analysis was carried out using STATA/SE software and Tukey's post hoc test was analyzed for pairwise comparisons of means with equal variances. The statistical analysis of the cytotoxicity test was reported concerning the control, \*  $p < 0.05$ .

### 3. Results

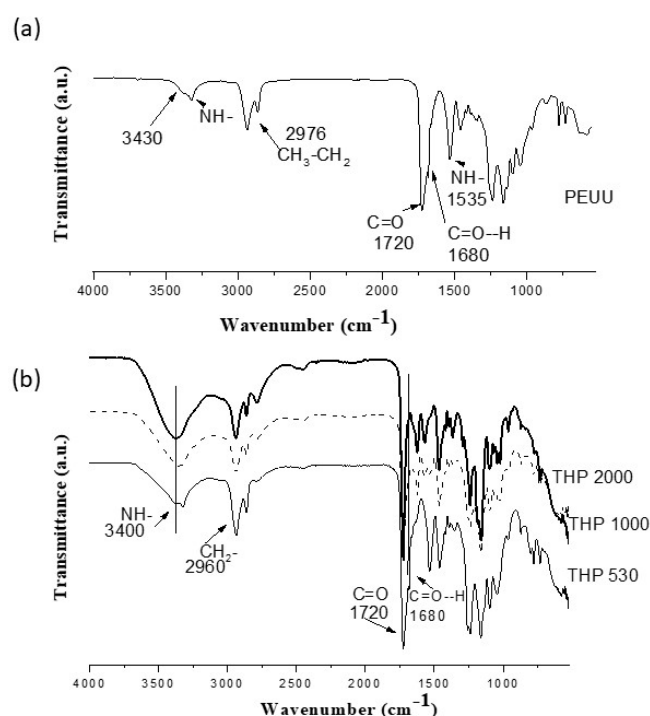
Segmented polyester (urea-urethanes) were obtained via two-stage polymerization method using polycaprolactone diol (PCL-d) as the soft segment and both hexamethylenediisocyanate (HMDI) and L-lysine-ethyl-ester-hydrochloride (LYS) as the hard segment.

Table 1 displays the codes and values for the contact angle and hardness of the PEUUs and hybrid materials (THPs). The molecular weight (Mw) and polydispersity (Mw/Mn) of PEUUs are also reported. As it can be seen in Table 1, the increase in the molecular weight of PEUUs directly influence the Vickers hardness values, due to the greater polymer chains formation and the low crystallinity, as discussed in the XRD section.

**Table 1.** Sample codes, contact angle and hardness of PEUUs and hybrid materials (THPs), and Mw and Mw/Mn of PEUUs.

Sample Codes of PEUUs	PEUUs Mw (g/mol)	PEUUs Mw/Mn	Contact Angle	Vickers Hardness (MPa)	Sample Codes of Hybrids	Contact Angle	Vickers Hardness (MPa)
PEUU <sub>530</sub>	27,600	1.2	70°	8	THP <sub>530</sub>	48°	10
PEUU <sub>1000</sub>	136,700	1.8	73°	35	THP <sub>1000</sub>	45°	50
PEUU <sub>2000</sub>	196,300	2.0	77°	48	THP <sub>2000</sub>	40°	60

Figure 1a shows a representative FT-IR spectrum of the PEUUs. At  $3320\text{ cm}^{-1}$ , a broad band due to the vibrations of hydrogen-bonded urea and urethane groups in the N-H groups is observed. The shoulder located at  $3430\text{ cm}^{-1}$  is due to the non-hydrogen bonded N-H groups related to the LYS, which hinders the molecular arrangement of the hard segment and promotes an asymmetric structure. The C=O absorption band located at  $1720\text{ cm}^{-1}$  from the ester groups and non-hydrogen bonded carbonyl groups (C=O-H) at  $1680\text{ cm}^{-1}$  are related to the PCL-d soft segment [19–21].



**Figure 1.** FT-IR spectra of the (a) PEUUs and (b) hybrid materials (THPs).

FT-IR spectra (Figure 1b) of the hybrid materials show the same bands as the PEUU spectrum described above. However, bands located at 3400 cm<sup>-1</sup> and 1680 cm<sup>-1</sup> due to the amine and carbonyl groups, respectively, are higher than those observed in PEUU. In addition, the broad bands located between 400 and 1000 cm<sup>-1</sup> may also be attributed to the Ti–O–Ti and Ti–OH bonds of the inorganic components [22,23].

The Raman spectra of the PEUUs (Figure 2a) peaks at 2919 cm<sup>-1</sup> and 1300 cm<sup>-1</sup> due to the CH<sub>2</sub>- groups in the polyurethanes; peaks at 1738 cm<sup>-1</sup> and 1676 cm<sup>-1</sup> are due to the ester in both carbonyl groups (C=O) and non-hydrogen linked groups (C=O–H), respectively. Furthermore, peaks observed at 1450 cm<sup>-1</sup>, 1100 cm<sup>-1</sup>, and 1085 cm<sup>-1</sup> are due to NH- groups, the C–O–C and C–C bonds, respectively [16,24]. The peaks at 240 cm<sup>-1</sup> and 320 cm<sup>-1</sup> are related to the polymer carbon skeleton.

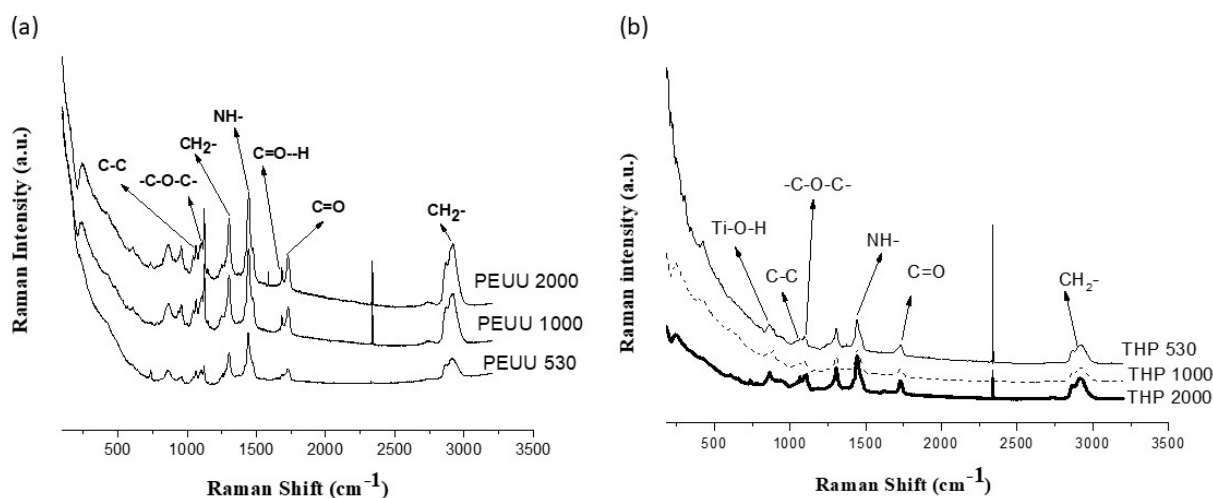


**Figure 2.** Raman spectra of the (a) PEUUs and (b) hybrid materials (THPs).

On the other hand, the contribution of the inorganic component (TiO<sub>2</sub>) is appreciated in the Raman spectra of the hybrid materials. Figure 2b shows weaker Raman peaks related

to the polymer matrix discussed before. However, some of them are shifted to a minor wavenumber, i.e., at  $1070\text{ cm}^{-1}$  and  $1095\text{ cm}^{-1}$ , due to the C–C and C–O–C groups, at  $1440\text{ cm}^{-1}$  and  $1730\text{ cm}^{-1}$  which is related to the NH- and C=O groups; also, the peak at  $1676\text{ cm}^{-1}$  of (C=O–H) is no longer observed. The peak located at  $860\text{ cm}^{-1}$  corresponds to the Ti–O–H groups [24]. These changes are related to the interaction between the organic and inorganic components.

It is well known that the sol–gel process helps to obtain vitreous materials at temperatures as low as room temperature and a subsequent heat treatment is required for their crystallization [25]. According to reference [26], titania was obtained using sol–gel process with similar synthesis conditions as in this work (acid medium, solvent and hydrolysis agent/titanium alkoxide ratio). They obtained a crosslinked network of vitreous titania, which was then heat-treated to produce the crystalline phases, anatase and rutile. In the present research, titania was obtained by applying the sol–gel reaction in a polymeric matrix (PEUUs) showing a vitreous structure, which will be discussed later.

A study [27] on the crystalline titania spin-coated on the poly-carbonate surface reports that the controlling the pH values during the sol–gel synthesis in a basic medium, to obtain the amorphous titania and the upcoming curing temperature, influence its crystallization. In the analysis of Raman spectra, the authors found weak bands at  $822\text{ cm}^{-1}$  and  $922\text{ cm}^{-1}$  due to Ti–OH groups related to the non-crystalline titania. Additionally, they observed that the increase in the pH during the synthesis of the amorphous titania results in the increase in crystalline phases after curing temperature, showing signals in the Raman spectra at  $150\text{ cm}^{-1}$  and  $508\text{ cm}^{-1}$  (anatase phase) and at  $442\text{ cm}^{-1}$  and  $692\text{ cm}^{-1}$  (rutile phase). No evidence of these signals is seen in the Raman spectra in Figure 2b, indicating that the crystalline phases are not present in the hybrid materials of this work since no heat-treatment was conducted. These observations are based on the results of the XRD analysis, which will be analyzed below.

Figure 3 shows the thermogravimetric curves of the PEUUs and THPs. The thermogram of PEUUs (Figure 3a) shows a weight loss only at  $\sim 300\text{ }^{\circ}\text{C}$ , attributed to polymer degradation. On the other hand, the thermograms of the THPs (Figure 3b) show three stages of weight loss. The first stage occurs below  $100\text{ }^{\circ}\text{C}$  with a weight loss of 5%, attributed to the loss of residual liquids (solvent and water from the polycondensation reactions) trapped in the hybrid network. The second stage occurs between  $100$  and  $200\text{ }^{\circ}\text{C}$  with a weight loss of  $\sim 20\%$ , corresponding to the loss of the unreacted monomers and the polymer chains of low molecular weight. The third stage is related to the initial degradation of the polymeric component (PEUUs), which takes place above  $200\text{ }^{\circ}\text{C}$  showing a weight loss of  $\sim 55\%$ . The complete decomposition of the polymer also is observed at  $\sim 500\text{ }^{\circ}\text{C}$  [28,29]. At the final thermal test ( $600\text{ }^{\circ}\text{C}$ ), the weight loss of both THP<sub>1000</sub> and THP<sub>2000</sub> hybrid materials is  $\sim 80\%$ , while the weight loss of THP<sub>530</sub> hybrid is  $\sim 90\%$ . As stated in the experimental section (Section 2.1.2), comprises a weight ratio of 80/20 of organic/inorganic components, hence, after the thermal test, the remaining weight corresponds to the inorganic component (TiO<sub>2</sub>) of the hybrid material. As can be seen, the remaining weight (20 wt.%) observed in THP<sub>1000</sub> and THP<sub>2000</sub> hybrids correspond to the weight of TiO<sub>2</sub> added during the synthesis. However, THP<sub>530</sub> remains at 10 wt.% (Figure 3b), indicating that not all TiO<sub>2</sub> added were effectively incorporated into the organic matrix due to the different molecular weight of the polymeric precursors (PCL and PEUUs). The observed remaining weight of titania could be related to the higher repeat units of ester and urea-urethane groups in the polymer, which leads to a higher interaction of the hydrogen bonds with the inorganic component. Therefore, THP<sub>1000</sub> and THP<sub>2000</sub> (with higher molecular weight) have a higher interaction with titania since a greater quantity of polar groups from polymeric matrix interacts with the inorganic component in the hybrid materials [16]. On the other hand, THP<sub>530</sub> has less polar groups available to interact, and consequently, loses part of the titania added during the synthesis, as can be seen in the thermogram in Figure 3b.

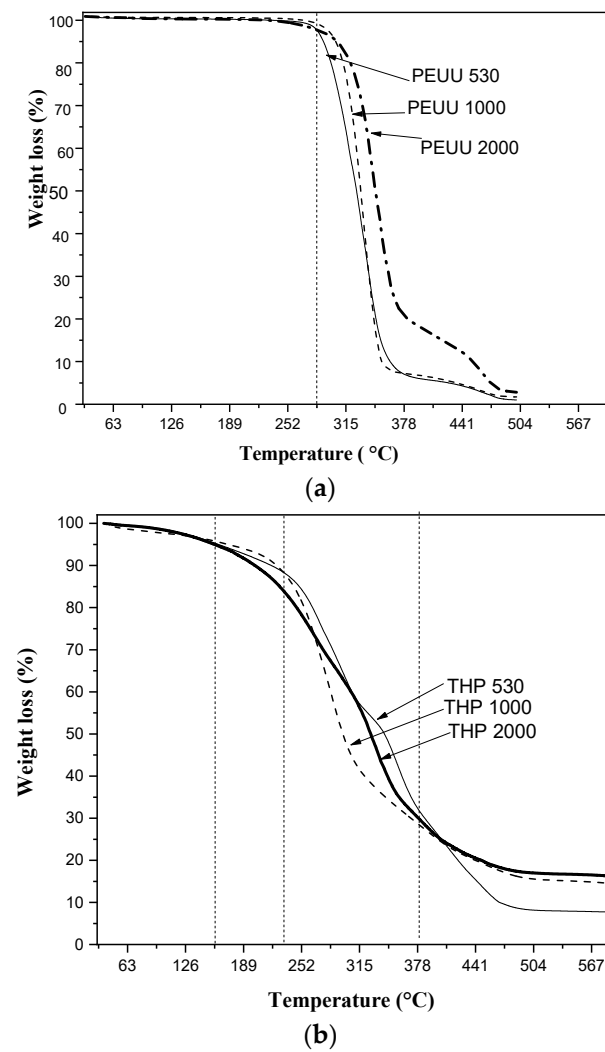


Figure 3. Thermograms of (a) PEUUs and (b) hybrid materials (THPs).

The thermal transition of the PEUUs and THPs are shown in Figure 4. In addition, Table 2 summarizes the thermal transitions of the hybrids (THPs).

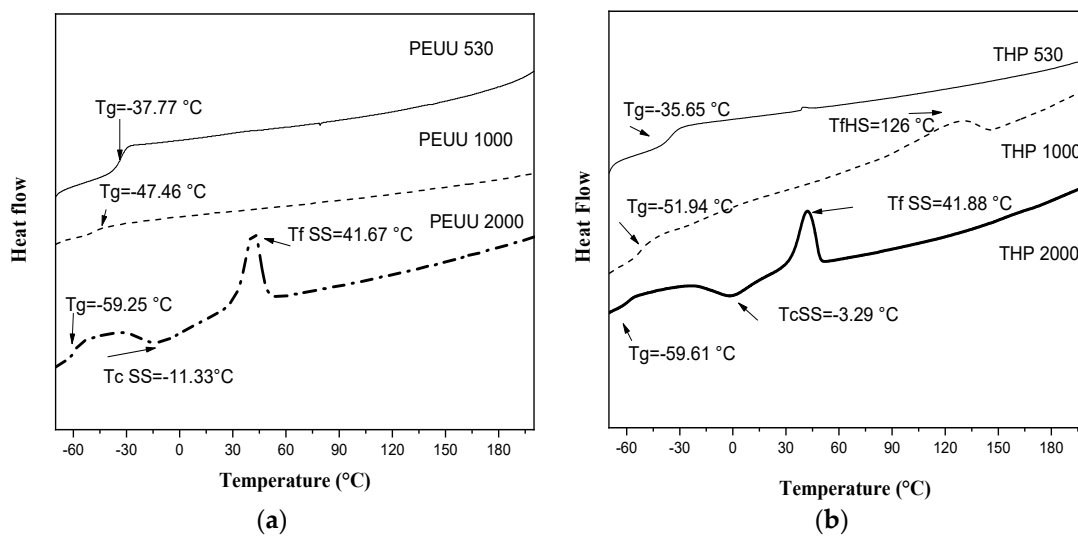


Figure 4. DSC of (a) PEUUs and (b) Hybrid materials (THPs).

**Table 2.** Thermal transitions of THPs.

Hybrid	Heat Sweep (−80–180 °C)			T <sub>g</sub>
	T <sub>c</sub> * SS	T <sub>f</sub> * SS	T <sub>f</sub> * HS	
THP <sub>530</sub>	—	—	—	−35.65
THP <sub>1000</sub>	—	—	126	−51.94
THP <sub>2000</sub>	−3.29	41.88	—	−59.61

\* SS = Soft segment. \* HS = Hard segment.

As mentioned above, the polyester-urea urethanes (PEUUs) are the polymeric component of the hybrid materials which is composed of soft (PCL of different molecular weight) and hard segment (diisocyanate and lysine). These segments could present a crystalline or amorphous structure [30]. As it is observed in Figure 4a, PEUU<sub>530</sub>, PEUU<sub>1000</sub> and PEUU<sub>2000</sub> show a glass transition temperature (T<sub>g</sub>) at −37.77 °C, −47.46 °C, and −59.25 °C, respectively, and it is related to the molecular weight of the PEUUs. No melting temperatures are observed for PEUU<sub>530</sub> and PEUU<sub>1000</sub>, but PEUU<sub>2000</sub> shows a crystallization temperature at −11.33 °C due to the soft segment (T<sub>c</sub> SS) and then the melting temperature is observed at 41.67 °C (T<sub>f</sub> SS). The crystallinity in the soft segment of PEUU<sub>2000</sub> is related to the major crystallinity in the PCL precursor with high molecular weight [31]. Furthermore, no thermal transitions were observed in the hard segment of this polymer. It could be explained in two ways: (1) the domains of the soft and hard segment were mixed in the first heating run, resulting in a single phase or, (2) the polymer showed a separation of the phases, one with rich domains in soft segment and other with rich domains in hard segment, as is discussed in other work [17].

On the other hand, Figure 4b shows the glass transition temperature at −35.65 °C, −51.94 °C, and −59.61 °C of the THP<sub>530</sub>, THP<sub>1000</sub>, and THP<sub>2000</sub> hybrid materials, respectively. Since the hybrid materials are composed of 80 wt.% of the polymer, similar thermal transitions of PEUUs (Figure 4a) are expected. As can be observed, T<sub>g</sub> value decreases as the molecular weight of the polymer increases. The THP<sub>1000</sub> hybrid shows a melting temperature at 126 °C due to the hard segment (T<sub>f</sub> HS), although this transition was not observed in its polymer precursor (PEUU<sub>1000</sub>). This could be attributed to the influence of the vitreous titania in the polymer matrix in which the titania interacts via hydrogen bonds with the hard segment domains. Finally, the crystallization (T<sub>c</sub>) and the melting (T<sub>f</sub>) temperatures of the soft segment in THP<sub>2000</sub> take place at −3.29 °C and 41.88 °C, respectively, corresponding to the thermal behavior of the polymer precursor (PEUU<sub>2000</sub>) in the hybrid material. As can be seen, the hybrid materials showed an increase in T<sub>g</sub> and a slight increase in T<sub>f</sub> values compared to the PEUUs precursors. It could be related to the inorganic components that interacts principally with polar groups (carbonyl and amine groups) via hydrogen bonds, as discussed when FT-IR (Figure 1) and Raman (Figure 2) spectroscopy were conducted. This interaction promotes a different rearrangement in the structure of the polymer chains [32]. Therefore, the thermal behavior could be improved with the presence of an inorganic phase.

The X-ray diffractograms of PEUUs and hybrid materials are shown in Figure 5.

The XRD patterns of PEUUs in Figure 5a show an amorphous halo with a maximum at ~22° in 2 theta, characteristic of low order arrangement materials. On the other hand, the XRD patterns of hybrid materials (Figure 5b) show a narrower amorphous halo, as described before, but a very low intensity peak at ~22° in 2 theta and a very small and narrow peak at ~38° in 2 theta is also observed. This could be related to the low order arrange of vitreous titania.

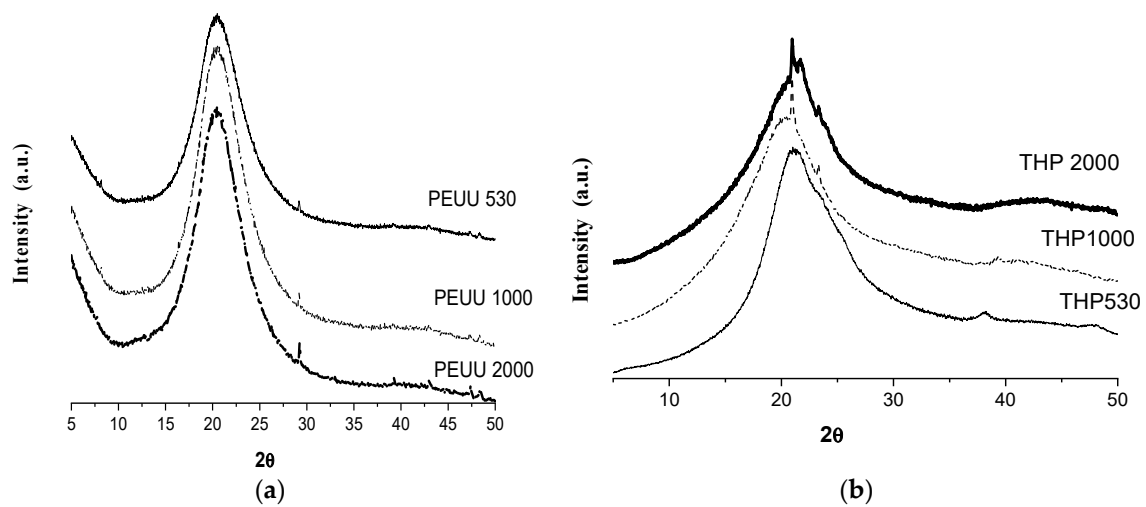


**Figure 5.** X-ray diffraction patterns of (a) PEUUs and (b) THPs.

The lack of crystallinity diffraction peaks related to the titania crystalline phases (rutile at  $27.4^\circ$ ,  $36.07^\circ$ ,  $39.17^\circ$ , and  $41.20^\circ$  and for anatase at  $25.27^\circ$ ,  $36.93^\circ$ ,  $37.78^\circ$ , and  $38.56^\circ$  in  $2\theta$ ) [33] is due to the presence of vitreous titania, as discussed in the FT-IR and Raman sections. Other authors have also reported obtaining a vitreous titania using the sol-gel method with similar synthesis conditions reported in this work; they also studied the phase transformations of the vitreous titania to anatase and rutile phases by heat treatment [26].

The SEM images of the morphology and the elemental mapping of Ti obtained using the EDX analysis of the hybrid materials are shown in Figure 6. As can be seen, the THP<sub>530</sub>, THP<sub>1000</sub>, and THP<sub>2000</sub> hybrid samples are wrinkled and dense solids with some agglomerates on their surface. Additionally, it is observed that TiO<sub>2</sub> is well-dispersed on the hybrid surfaces.

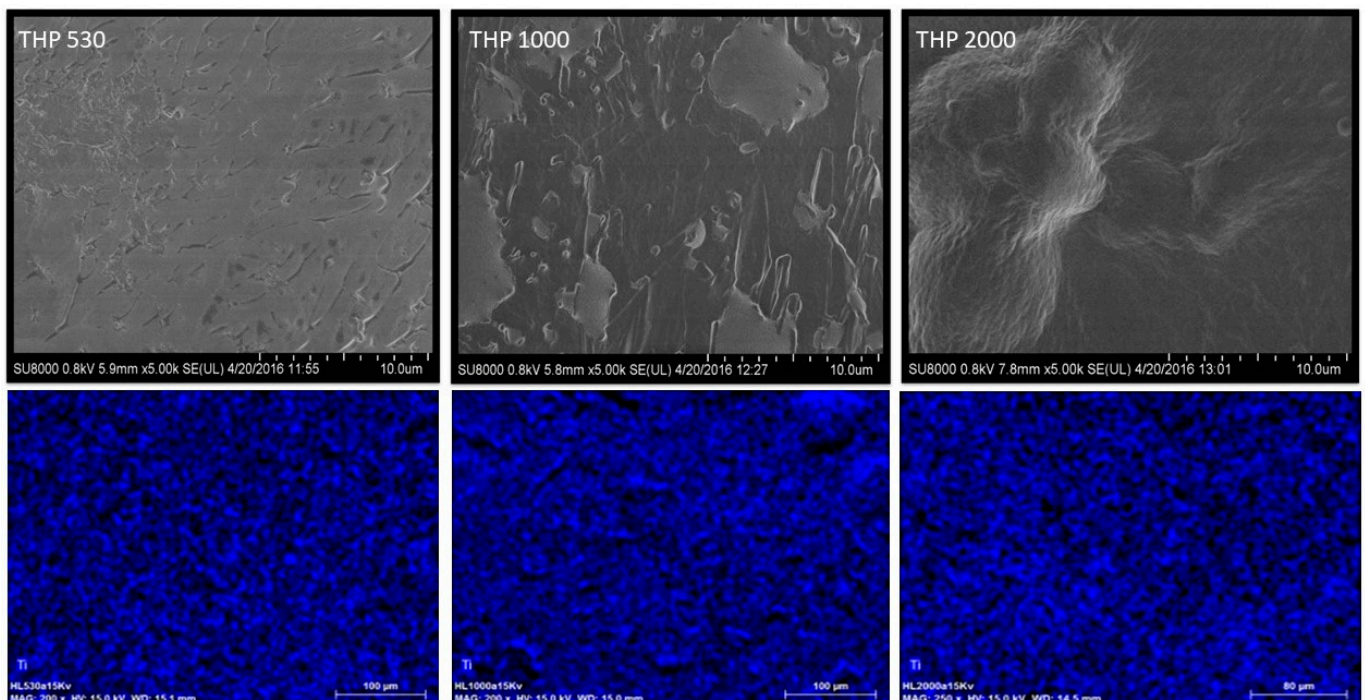


**Figure 6.** Morphology of the hybrid materials obtained using SEM and elemental Ti distribution from EDX mapping.

On the other hand, the analysis of the degradability test was carried out by means of the changes in weight of the hybrid samples after being immersed in the buffer solution (PBS), and the variation of the pH values of this solution at different test times are shown in Figure 7.

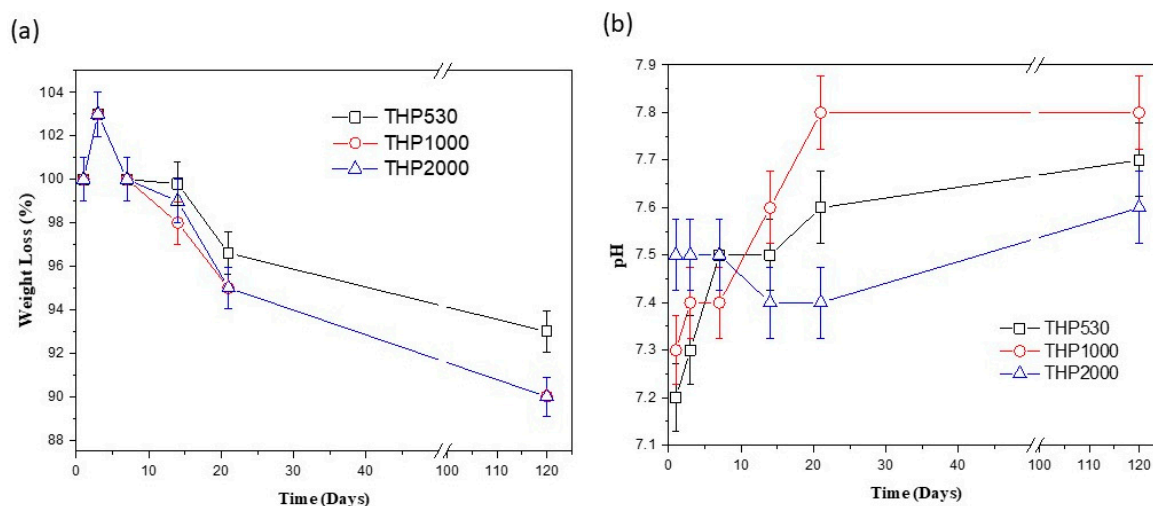


**Figure 7.** (a) Change in weight of THPs after being immersed in PBS and (b) pH variation of PBS at each time of test. Physiological conditions were used.

The tendency towards weight loss exhibited by the hybrid materials is similar in all the three cases. On the first day, the weight of the hybrids increases due to the absorption of the PBS solution, and on the third day, they experience a gradual weight loss. The total weight loss of the three hybrids is  $\sim 10\%$  at 120 days of testing.

The pH values observed in the first three days of testing are related to the release of residual reagents and solvents trapped in the hybrid network. After this time, the pH shows a value of 7.4–7.5, which remains until 14 days of testing. Then, the pH value increases slightly without exceeding a pH value of 7.8 due to the amine groups of the hybrids released into the solution. This fact shows a low degradation of hybrid materials.

The results of the cell viability (CV) assay for the three hybrid materials and for the control (TERMANOX) at 24 h are shown in Figure 8. The THP<sub>530</sub> and THP<sub>1000</sub> hybrid materials present greater cell viability ( $\geq 80\%$ ) than the THP<sub>2000</sub> hybrid ( $\geq 70\%$ ). However, the observed cell viability values indicate that the hybrids are non-cytotoxic materials, as mentioned in other works with similar values of cell viability [34,35]. The lower cell viability of THP<sub>2000</sub> could be related to the amount of residual solvent trapped in the hybrid. However, it is assumed that after a few days, the residuals will be eliminated, according to the results of the degradation test. Furthermore, cell proliferation begins on the first day of the *in vitro* test.

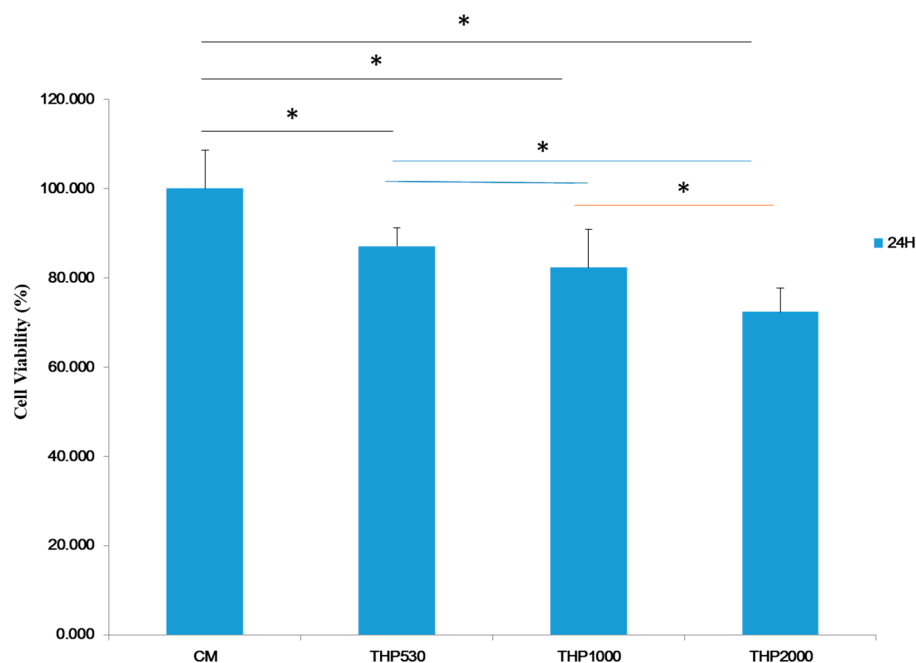


**Figure 8.** Cell viability of the hybrid materials at 24 h using an osteoblastic cell line. One-way ANOVA (\*) indicates statistical difference from the control  $p < 0.05$ .

#### 4. Discussion

In a previous work [17], the effect of the chemical nature of both the hard segment and the soft segment of polyurea-urethanes on the chemical, mechanical and biological properties of polymers was analyzed. The obtained polyurea-urethanes showed good mechanical behavior and excellent biostability. Furthermore, in the present work, the hybridization of these polymers with titania and synthetization of the THPs via the sol-gel process was demonstrated using FT-IR and RAMAN analysis wherein the non-hydrogen bonded urea groups decrease, and the linked carbonyl groups increases. This could be related to the new hydrogen bonds formed between the amine and carbonyl groups from the polymer and the inorganic component. Such interactions between organic and inorganic component were thought to be responsible for forming Class I hybrids, as described in the literature [36,37]. In addition, the contribution of titania is noted in the Raman peak at  $860\text{ cm}^{-1}$  due to Ti-O-H bonds. The interactions between inorganic and organic components in the hybrid directly influence important properties of the materials, such as thermal and mechanical properties.

The Vickers hardness values (Table 1) of PEUU<sub>530</sub>, PEUU<sub>1000</sub> and PEUU<sub>2000</sub> are 8, 35 and 48 MPa, respectively, while the Vickers hardness values of hybrid materials are 10, 50 y 60 MPa for THP<sub>530</sub>, THP<sub>1000</sub>, and THP<sub>2000</sub>, respectively, showing values 20% higher than the respective PEUUs. This increment is attributed to the presence of the vitreous titania which is well dispersed into the polymer matrix of the hybrids. Additionally, the hardness of polymers and hybrid materials depends on the molecular weight of their respective precursor: as the molecular weight of the precursor increases, the hardness also increases in both polymers and hybrid materials.

Hydrophilicity is a desirable property for materials interacting with cells for tissue regeneration, as shown in reference [38], in which the authors reported that an increment in the contact angle increases cell adhesion and proliferation.

The degradation in an aqueous medium and the release of non-toxic products are necessary properties of biomaterials intended for tissue regeneration applications. In the present work, the hybrid materials show a weight loss of ~10% after being immersed in PBS for 120 days.

The introduction of the inorganic phase (TiO<sub>2</sub>) in the polymeric matrix through sol-gel reactions improve the mechanical, thermal, and biological properties of the hy-

brid materials. Additionally, titania is non-cytotoxic and is well known to promote osteoconductivity [16,39,40], as seen in the cell viability test using the human osteoblast cell line presented in Figure 8.

Additionally, the inorganic phase can be introduced as particles or synthesized in situ with the organic phase in composite and hybrid materials providing the possibility to tailor the mechanical and physicochemical properties of materials for different applications. Related works [41–43] reported materials based on polyurethanes with the addition of particles or in situ synthesis of titania in different concentrations to improve the properties in the final materials for various applications. In reference [44], the authors synthesized in situ composite materials based on polyurethanes and commercial TiO<sub>2</sub> particles. They mentioned that TiO<sub>2</sub> interacts with the hydrogen from carbonyl groups of the polymer and analyzed its different properties. They found that the thermal and mechanical properties improved with the introduction of TiO<sub>2</sub>.

In our work, hybrid materials were obtained through the in situ reaction of vitreous TiO<sub>2</sub> and PEUU using the sol–gel process. For this purpose, hydrolysis–condensation reactions were carried out within the polymer, which resulted in a strong interaction between the organic and inorganic phases, providing materials with better thermal and mechanical behavior and promising biological results.

## 5. Conclusions

A novel material based on polyester (urea-urethanes) and titania was synthesized using the sol–gel reaction. The strong interaction between the organic and inorganic phases influences thermal and mechanical properties. Additionally, the surface of the materials is more hydrophilic, and the in vitro cytotoxicity of hybrid residues was analyzed at 24 h, which showed that they were non-cytotoxic to human osteoblast cells.

**Author Contributions:** Conceptualization, D.M.G.-G. and R.J.-G.; Methodology, D.M.G.-G. and Á.M.-F.; Software, D.A.S.-T.; Validation, Á.M.-F. and L.T.-J.; Formal Analysis, Á.M.-F. and D.M.G.-G.; Investigation, D.M.G.-G.; Resources, Á.M.-F. and L.T.-J.; Data Curation, D.A.S.-T.; Writing—Original Draft Preparation, D.M.G.-G.; Writing—Review and Editing, L.M.R.-L. and L.T.-J.; Visualization, R.J.-G.; Supervision, Á.M.-F. and L.T.-J.; Project Administration, L.T.-J.; Funding Acquisition, L.T.-J. and L.M.R.-L. All authors have read and agreed to the published version of the manuscript.

**Funding:** This work was supported by project PID2020-119047RB-I00, financed by Spanish Ministerio de Ciencia e Innovación (MCIN/AEI/10.13039/501100011033/), CONACYT and IPN-SIP/20201294 from Mexico for the fellowship grant number 393020 and DPI 2017-90147-R from MINECO-AEI, Spain for the fund.

**Institutional Review Board Statement:** Not applicable.

**Data Availability Statement:** The data that support the findings of this study are available on request from the corresponding author.

**Acknowledgments:** D.M. Gonzalez-Garcia thank CONACYT and IPN-SIP/20201294 from Mexico for the fellowship grant and thank DPI 2017-90147-R from MINECO-AEI, Spain and PID2020-119047RB-I00, financed by Spanish Ministerio de Ciencia e Innovación (MCIN/AEI/10.13039/501100011033/) for the fund. Additionally, the authors thank Mar Fernandez Gutierrez and Rosa Ana Ramirez Jimenez for helping with the biological characterization and thank the ICTP in Madrid for the technical assistance.

**Conflicts of Interest:** The authors declare no conflict of interest.

## References

1. Sánchez-Téllez, D.A.; Téllez-Jurado, L.; Rodríguez-Lorenzo, L.M.; Mazo, M.A.; Rubio, J.; Tamayo, A. Surface effects on the degradation mechanism of bioactive PDMS-SiO<sub>2</sub>-CaO-P<sub>2</sub>O<sub>5</sub> hybrid materials intended for bone regeneration. *Ceram. Int.* **2017**, *43*, 476–483. [[CrossRef](#)]
2. Sanchez, C.; Shea, K.J.; Kitagawa, S. Recent progress in hybrid materials science. *Chem. Soc. Rev.* **2011**, *40*, 471–472. [[CrossRef](#)]
3. Abalymov, A.; Parakhonskiy, B.; Skirtach, A.G. Polymer-and hybrid-based biomaterials for interstitial, connective, vascular, nerve, visceral and musculoskeletal tissue engineering. *Polymers* **2020**, *12*, 620. [[CrossRef](#)] [[PubMed](#)]

4. Rubio Hernández-Sampelayo, A.; Navarro, R.; Marcos-Fernández, Á. Preparation of High Molecular Weight Poly (urethane-urea)s Bearing Deactivated Diamines. *Polymers* **2021**, *13*, 1914. [[CrossRef](#)] [[PubMed](#)]
5. Kishan, A.P.; Wilems, T.; Mohiuddin, S.; Cosgriff-Hernandez, E.M. Synthesis and characterization of plug-and-play polyurethane urea elastomers as biodegradable matrixes for tissue engineering applications. *ACS Biomater. Sci. Eng.* **2017**, *3*, 3493–3502. [[CrossRef](#)] [[PubMed](#)]
6. Szczepańczyk, P.; Szlachta, M.; Złocista-Szewczyk, N.; Chłopek, J.; Pielichowska, K. Recent developments in polyurethane-based materials for bone tissue engineering. *Polymers* **2021**, *13*, 946. [[CrossRef](#)]
7. Fernando, S.; McEnery, M.; Guelcher, S. Polyurethanes for bone tissue engineering. *Adv. Polyurethane Biomater.* **2016**, 481–501.
8. Miyazaki, T.; Imanaka, S.; Akaike, J. Relationship between valence of titania and apatite mineralization behavior in simulated body environment. *J. Am. Ceram. Soc.* **2021**, *104*, 3545–3553. [[CrossRef](#)]
9. Catauro, M.; Bollino, F.; Papale, F.; Lamanna, G. TiO<sub>2</sub>/pcl hybrid layers prepared via sol-gel dip coating for the surface modification of titanium implants: Characterization and bioactivity evaluation. *Appl. Mech. Mater.* **2015**, *760*, 353–358. [[CrossRef](#)]
10. Xu, Y.; Wen, W.; Wu, J.-M. Titania nanowires functionalized polyester fabrics with enhanced photocatalytic and antibacterial performances. *J. Hazard. Mater.* **2018**, *343*, 285–297. [[CrossRef](#)]
11. Eddy, D.R.; Luthfiah, A.; Permana, M.D.; Deawati, Y.; Firdaus, M.L.; Rahayu, I.; Izumi, Y. Rapid Probing of Self-Cleaning Activity on Polyester Coated by Titania–Natural Silica Nanocomposite Using Digital Image-Based Colorimetry. *ACS Omega* **2023**, *8*, 7858–7867. [[CrossRef](#)]
12. Hara, S.; Aisu, J.; Nishizaki, Y.; Kato, H.; Sanae, G.; Kurebayashi, S.; Shimizu, S.; Ikake, H. Bulk structure of poly (ethylene glycol)/Titania hybrid system and the evaluation of their influence on apatite growth using simulated body fluid (SBF). *Polym. Test.* **2021**, *94*, 106984. [[CrossRef](#)]
13. Al Sagheer, F.; Ahmad, Z. Preparation and characterization of chemically bonded aramid-titania hybrids using isocyanatopropyltrimethoxysilane. *J. Sol-Gel Sci. Technol.* **2013**, *65*, 243–254. [[CrossRef](#)]
14. Chen, Y.; Zhou, S.; Gu, G.; Wu, L. Microstructure and properties of polyester-based polyurethane/titania hybrid films prepared by sol–gel process. *Polymer* **2006**, *47*, 1640–1648. [[CrossRef](#)]
15. Chen, Q.; Miyaji, F.; Kokubo, T.; Nakamura, T. Apatite formation on PDMS-modified CaO–SiO<sub>2</sub>–TiO<sub>2</sub> hybrids prepared by sol–gel process. *Biomaterials* **1999**, *20*, 1127–1132. [[CrossRef](#)]
16. González-García, D.M.; Jurado, L.T.; Jiménez-Gallegos, R.; Rodríguez-Lorenzo, L.M. Novel non-cytotoxic, bioactive and biodegradable hybrid materials based on polyurethanes/TiO<sub>2</sub> for biomedical applications. *Mater. Sci. Eng. C* **2017**, *75*, 375–384. [[CrossRef](#)]
17. González-García, D.M.; Marcos-Fernández, Á.; Rodríguez-Lorenzo, L.M.; Jiménez-Gallegos, R.; Vargas-Becerril, N.; Téllez-Jurado, L. Synthesis and in vitro cytocompatibility of segmented poly (ester-urethane)s and poly (ester-urea-urethane)s for bone tissue engineering. *Polymers* **2018**, *10*, 991. [[CrossRef](#)]
18. Abraham, G.A.; Marcos Fernández, A.; San Román, J. Bioresorbable poly (ester-ether urethane)s from L-lysine diisocyanate and triblock copolymers with different hydrophilic character. *J. Biomed. Mater. Res. Part A* **2006**, *76*, 729–736. [[CrossRef](#)]
19. Báez, J.E.; Ramírez, D.; Valentín, J.L.; Marcos-Fernández, A.N. Biodegradable poly (ester–urethane–amide)s based on poly ( $\epsilon$ -caprolactone) and diamide–diol chain extenders with crystalline hard segments: Synthesis and characterization. *Macromolecules* **2012**, *45*, 6966–6980. [[CrossRef](#)]
20. Garrett, J.; Runt, J.; Lin, J. Microphase separation of segmented poly (urethane urea) block copolymers. *Macromolecules* **2000**, *33*, 6353–6359. [[CrossRef](#)]
21. Boerio, F.; Koenig, J. Vibrational spectroscopy of polymers. *J. Macromol. Sci. Rev. Macromol. Chem.* **1972**, *7*, 209–249. [[CrossRef](#)]
22. Yang, C.; Tang, Y.; Lam, W.; Lu, W.W.; Gao, P.; Zhao, C.; Yuen, M. Moisture-cured elastomeric transparent UV and X-ray shielding organic–inorganic hybrids. *J. Mater. Sci.* **2010**, *45*, 3588–3594. [[CrossRef](#)]
23. Ochoa, Y.; Ortégón, Y.; Vargas, M.; Páez, J. Síntesis de TiO<sub>2</sub>, fase anatasa, por el método Pechini. *Supl. De La Rev. Latinoam. De Metal. Y Mater.* **2009**, *3*, 931–937.
24. Pignanelli, F.; Romero, M.; Castiglioni, J.; Faccio, R.; Mombrú, A.W. Novel synergistic in situ synthesis of lithium-ion poly (ethylene citrate)-TiO<sub>2</sub> nanocomposites as promising fluorine-free solid polymer electrolytes for lithium batteries. *J. Phys. Chem. Solids* **2019**, *135*, 109082. [[CrossRef](#)]
25. Brinker, C.J.; Scherer, G.W. *Sol-Gel Science: The Physics and Chemistry of Sol-Gel Processing*; Academic Press: Cambridge, MA, USA, 2013.
26. Ding, X.-Z.; Qi, Z.-Z.; He, Y.-Z. Effect of hydrolysis water on the preparation of nano-crystalline titania powders via a sol-gel process. *J. Mater. Sci. Lett.* **1995**, *14*, 21–22. [[CrossRef](#)]
27. Yaghoubi, H.; Dayerizadeh, A.; Han, S.; Mulaj, M.; Gao, W.; Li, X.; Muschol, M.; Ma, S.; Takshi, A. The effect of surfactant-free TiO<sub>2</sub> surface hydroxyl groups on physicochemical, optical and self-cleaning properties of developed coatings on polycarbonate. *J. Phys. D Appl. Phys.* **2013**, *46*, 505316. [[CrossRef](#)]
28. Javni, I.; Petrović, Z.S.; Guo, A.; Fuller, R. Thermal stability of polyurethanes based on vegetable oils. *J. Appl. Polym. Sci.* **2000**, *77*, 1723–1734. [[CrossRef](#)]
29. Jiménez-Gallegos, R.; Téllez-Jurado, L.; Rodríguez-Lorenzo, L.M. Modulation of the hydrophilic character and influence on the biocompatibility of polyurethane-siloxane based hybrids. *Bol. Soc. Esp. Ceram. Vidr.* **2011**, *50*, 1–8. [[CrossRef](#)]
30. Oertel, G. *Polyurethane Handbook*, 2nd ed.; Hanser: Munich, Germany, 1993.

31. Bagdi, K.; Molnár, K.; Sajo, I.; Pukánszky, B. Specific interactions, structure and properties in segmented polyurethane elastomers. *Express Polym. Lett.* **2011**, *5*, 417–427. [[CrossRef](#)]
32. Zhang, S.; Jiang, J.; Yang, C.; Chen, M.; Liu, X. Facile synthesis of waterborne UV-curable polyurethane/silica nanocomposites and morphology, physical properties of its nanostructured films. *Prog. Org. Coat.* **2011**, *70*, 1–8. [[CrossRef](#)]
33. Cheng, H.; Ma, J.; Zhao, Z.; Qi, L. Hydrothermal preparation of uniform nanosize rutile and anatase particles. *Chem. Mater.* **1995**, *7*, 663–671. [[CrossRef](#)]
34. Catauro, M.; Renella, R.; Papale, F.; Cipriotti, S.V. Investigation of bioactivity, biocompatibility and thermal behavior of sol–gel silica glass containing a high PEG percentage. *Mater. Sci. Eng. C* **2016**, *61*, 51–55. [[CrossRef](#)]
35. Catauro, M.; Papale, F.; Bollino, F.; Gallicchio, M.; Pacifico, S. Biological evaluation of zirconia/PEG hybrid materials synthesized via sol–gel technique. *Mater. Sci. Eng. C* **2014**, *40*, 253–259. [[CrossRef](#)]
36. Owens, G.J.; Singh, R.K.; Foroutan, F.; Alqaysi, M.; Han, C.-M.; Mahapatra, C.; Kim, H.-W.; Knowles, J.C. Sol–gel based materials for biomedical applications. *Prog. Mater. Sci.* **2016**, *77*, 1–79. [[CrossRef](#)]
37. Sanchez, C.; Ribot, F. Design of hybrid organic-inorganic materials synthesized via sol-gel chemistry. *N. J. Chem.* **1994**, *18*, 1007–1047.
38. Gorna, K.; Gogolewski, S. Molecular stability, mechanical properties, surface characteristics and sterility of biodegradable polyurethanes treated with low-temperature plasma. *Polym. Degrad. Stab.* **2003**, *79*, 475–485. [[CrossRef](#)]
39. Catauro, M.; Bollino, F.; Papale, F.; Marciano, S.; Pacifico, S. TiO<sub>2</sub>/PCL hybrid materials synthesized via sol–gel technique for biomedical applications. *Mater. Sci. Eng. C* **2015**, *47*, 135–141. [[CrossRef](#)] [[PubMed](#)]
40. Catauro, M.; Papale, F.; Bollino, F. Characterization and biological properties of TiO<sub>2</sub>/PCL hybrid layers prepared via sol–gel dip coating for surface modification of titanium implants. *J. Non-Cryst. Solids* **2015**, *415*, 9–15. [[CrossRef](#)]
41. Che, X.-C.; Jin, Y.-Z.; Lee, Y.-S. Preparation of nano-TiO<sub>2</sub>/polyurethane emulsions via in situ RAFT polymerization. *Prog. Org. Coat.* **2010**, *69*, 534–538. [[CrossRef](#)]
42. Chen, J.; Zhou, Y.; Nan, Q.; Ye, X.; Sun, Y.; Zhang, F.; Wang, Z. Preparation and properties of optically active polyurethane/TiO<sub>2</sub> nanocomposites derived from optically pure 1, 1'-binaphthyl. *Eur. Polym. J.* **2007**, *43*, 4151–4159. [[CrossRef](#)]
43. Mirabedini, S.; Sabzi, M.; Zohuriaan-Mehr, J.; Atai, M.; Behzadnasab, M. Weathering performance of the polyurethane nanocomposite coatings containing silane treated TiO<sub>2</sub> nanoparticles. *Appl. Surf. Sci.* **2011**, *257*, 4196–4203. [[CrossRef](#)]
44. Demétrio da Silva, V.; dos Santos, L.M.; Subda, S.M.; Ligabue, R.; Seferin, M.; Carone, C.L.; Einloft, S. Synthesis and characterization of polyurethane/titanium dioxide nanocomposites obtained by in situ polymerization. *Polym. Bull.* **2013**, *70*, 1819–1833. [[CrossRef](#)]

**Disclaimer/Publisher's Note:** The statements, opinions and data contained in all publications are solely those of the individual author(s) and contributor(s) and not of MDPI and/or the editor(s). MDPI and/or the editor(s) disclaim responsibility for any injury to people or property resulting from any ideas, methods, instructions or products referred to in the content.